

# Application of Reliability and Quality Methods to Improving Mean Time Between Failures of Machine Tool Cooling System

Chun-Hao Chen<sup>1</sup> and Kun-Ying Li<sup>2\*</sup>

<sup>1</sup>Graduate Institute of Precision Manufacturing, National Chin-Yi University of Technology,  
No. 57, Sec. 2, Zhongshan Rd., Taiping Dist., Taichung 41170, Taiwan

<sup>2</sup>Department of Intelligent Automation Engineering, National Chin-Yi University of Technology,  
No. 57, Sec. 2, Zhongshan Rd., Taiping Dist., Taichung 41170, Taiwan

(Received August 3, 2023; accepted November 7, 2023)

**Keywords:** reliability, MTBF, machine tool, cooling system

The thermal error of a machine tool can be regarded as an important index of machining accuracy. Such an error is reproducible and stable, meaning that machine tools can be easily maintained by thermal compensation, ensuring a long-term good machining quality. In this study, reliability engineering was applied to increase the mean time between failures (MTBF) of a cooling system to maintain the structure temperature and accuracy, and the MTBF was increased from 3787 h to more than 23041 h. In addition, the Taguchi method was used with the finite element method and multivariate regression analysis to obtain the optimal cooling conditions to reduce thermal deformation and stabilize the structure temperature. The variation of the temperature of the machine tool structure was improved from  $\pm 0.517$  to  $\pm 0.367$  °C, a reduction of 29%.

## 1. Introduction

Machining errors of a machine tool can be caused by thermal deformation.<sup>(1)</sup> Under the dynamic operation of a machine tool, the frictional heat generated by the high-speed rotation of the bearings in a spindle causes thermal deformation, reducing the machining accuracy. Some machining industries have adopted thermal compensation and design methods to improve the machining accuracy, such as thermal insulation, heat balance design, and cooling methods; cooling methods reduce the generation of heat before a thermal error occurs. The effect of a cooling method for reducing the error is better than those of the thermal compensation and design methods; however, the design of the cooling channel structure is complicated. Factors affecting the accuracy of machine tools include static geometric and dynamic thermal errors, the tool wear and thermal deformation of the workpiece during machining, and variations in the external working environment. To reduce the thermal deformation of a spindle, Vyroubal<sup>(2)</sup> conducted a simulation analysis and compensated for the axial thermal deformation of the spindle to improve the machining precision. Huang *et al.*<sup>(3)</sup> designed a cooling channel to

---

\*Corresponding author: e-mail: [likunying@ncut.edu.tw](mailto:likunying@ncut.edu.tw)  
<https://doi.org/10.18494/SAM4689>

increase the efficiency of spindle cooling. Liu *et al.*<sup>(4)</sup> proposed a differentiated multiloop recirculation system for precision machine tools. The system can adjust the temperature and flow according to the machine tool part, thus effectively controlling the temperature field and thermal error. This system reduced the thermal error by up to 64.3% compared with that of a traditional cooling system. Ngo *et al.*<sup>(5)</sup> developed a thermoelectric cooling module as an alternative to a traditional air cooling system, in which the temperature and thermal displacement of small built-in spindles are controlled, reducing the time to reach a steady-state temperature by 47%. Li *et al.*<sup>(6)</sup> adjusted the oil circulation flow according to the machining load and rotation speed of the spindle to remove the heat generated from the spindle. They also built a mathematical model of cooling oil flow based on the speed and torque of the spindle. In their study, the machining accuracy was improved by 34%. Tang *et al.*<sup>(7)</sup> proposed a novel convex water-cooling flow channel based on the rectangular water-cooling flow channel of its built-in spindle. On the basis of the results of numerical simulation, they built a fluid–solid coupling analysis model for the water cooling of the spindle. The convex structure increased the convective heat transfer of the fluid and improved the cooling effect. Xia *et al.*<sup>(8)</sup> designed a cooling water jacket with a novel fractal tree network flow channel based on fractal theory, which they compared with a traditional cooling water jacket with a spiral flow channel. The proposed water jacket had a lower pressure drop, a more uniform temperature field distribution, and a larger performance coefficient and over twice the cooling efficiency than the channel cooling water jacket with the spiral flow. Dai *et al.*<sup>(9)</sup> used a novel spiral cooling system to control the temperature of a built-in high-speed spindle. They analyzed the internal heat transfer mechanism of the spindle and used the gradient descent method to optimize the heat transfer on the basis of experimental data. The reliability of the gradient descent method for simulation was verified, and the cost of developing future built-in spindles was reduced effectively.

Machine tools made in Taiwan have comparable functional specifications to imported machine tools, and Taiwanese manufacturers have better after-sales service than importers as well as lower prices. However, imported machine tools have a higher accuracy, a greater reliability, and a longer service lifetime. As a result, Taiwan's machine tool industry is positioned in the mid-to-low end of the market. The average unit price of products in Taiwan is about half of those in Germany and Switzerland and about two-thirds of that in Japan. Keller *et al.*<sup>(10)</sup> studied the reliability and maintainability of machine tools, and spent three years analyzing the field failure data of 35 machine tools within their warranty period. They found that the lognormal and Weibull distributions were effective in defining the time between failures. Ran *et al.*<sup>(11)</sup> believe that it is difficult to analyze the overall reliability of machine tools. To improve the stability and reliability of machine processing, a meta-action unit (Action unit, MU) was proposed by the function–motion–action (FMA) decomposition method to improve the processing stability and reliability of the machine tools. Wang *et al.*<sup>(12)</sup> proposed an accuracy analysis method to evaluate the accuracy and predict the lifetime of a milling machine. In this method, an analytic hierarchy process derived a subjective weight through the established function–motion–action–error hierarchy. Finally, the comprehensive weight of the error index and sensitivity analysis were used to predict the lifetime and evaluate the accuracy of the milling machine. Li *et al.*<sup>(13)</sup> used the Bayesian network model to analyze the reliability of the main drive system (MDS) of a large

boring machine tool. The reliability and mean failure time of the MDS and the subsystems were predicted with an error of 10.5%. Zhang *et al.*<sup>(14)</sup> proposed a geometric error estimation method based on the Rackwitz–Fiessler theory that considers geometric errors, thermal errors, and tool wear. They built reliability and sensitivity models to improve the machining accuracy and reliability of machine tools. Anikeeva *et al.*<sup>(15)</sup> developed a decision-making technology for evaluating the reliability and machining quality of machine tools. They reduced the difference in accuracy between machine tools by identifying the relationship between the accuracy parameters of the machined parts and those of a machine tool. Cheng *et al.*<sup>(16)</sup> used multibody system theory to develop an error allocation method to optimize the distribution of manufacturing and assembly tolerances. They built a volumetric error model to compensate for the errors generated during the operation of a machine tool, improving the machining accuracy and reliability of five-axis machine tools. Zhang *et al.*<sup>(17)</sup> proposed a method of evaluating machining accuracy that simultaneously considers geometric and vibration errors, thus ensuring the long-term high machining accuracy and reliability of five-axis machining tools. In this study, we adopted the DIS-MCS sampling method to establish a machining accuracy reliability model. The application results showed the accuracy and competitive performance of the method. Guo *et al.*<sup>(18)</sup> used the accelerated lifetime test method to evaluate reliability and proposed a multiaxis loading device to simulate the overload of a feed system during machine tool operation. The results showed that the experimental cost of ensuring reliability was reduced, with an error of less than 10% between the experiment and the simulation. Liu *et al.*<sup>(19)</sup> utilized the operating data of a grinding machine to build a model of each of its subsystems. They optimized the models through corrected gray correlation. They found that point estimates based on the Monte Carlo algorithm had a higher accuracy reliability model than the traditional method of fitting the entire machine. The Monte Carlo algorithm can be used to assess the machine's reliability in reliability design.

In this study, reliability engineering was applied to increase the mean time between failures (MTBF) of a cooling system, and the Taguchi method was used to optimize the cooling conditions and decrease the temperature of a machine tool structure.

## 2. Experimental Equipment and Methods

### 2.1 Equipment for cooling experiment

About 70% of the accuracy errors in machine tools are caused by thermal error. Therefore, cooling channels are introduced into the structural design. An oil circulation mechanism is used to suppress the effect of thermal deformation. A cooling experiment was conducted on a single-axis feed platform to investigate the behavior of a structure under thermal deformation and the coolant flow rate that suppressed the thermal deformation. Figure 1 shows photographs of the experimental cooling system and the single-axis feed platform, and the positions of the temperature measurement points.

In the experiment, the temperature change of the single-axis feed platform was measured using a Graphtec GL820 measurement recorder with a Kyowa strain measurement system. The temperature of the single-axis feed platform was measured using a thermometer (PT100). All

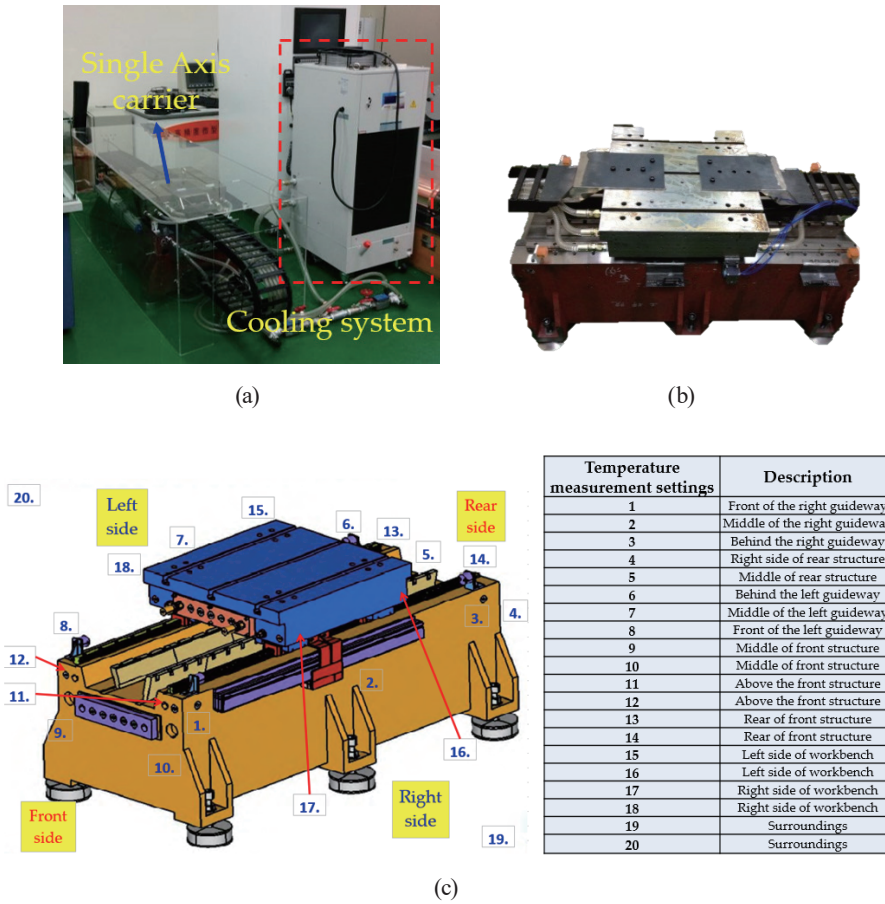


Fig. 1. (Color online) Experimental platform: (a) cooling system, (b) single-axis feed platform, and (c) temperature measurement positions.

measured temperature data were recorded in the GL820 recorder and used to analyze the experimental results. Figure 2 shows the measurement equipment used in this study.

### 2.2 Methodology

The cooling oil was circulated to suppress the heat source of the structure. In this study, we aim to control the structural temperature changes and improve the MTBF value. Assuming that the reliability target of the cooling system is  $R_s$ , we use a serial exponential distribution model as described by Eqs. (1)–(3) as the reliability, where  $\theta$  is the MTBF and  $\lambda$  is the failure rate, which has a reciprocal relationship with  $\theta$ .

$$R_{s(t)} = e^{(-\lambda s \cdot t)} = e^{(-t/\theta_s)} \tag{1}$$

$$\lambda_s = 1 / \theta_s \tag{2}$$

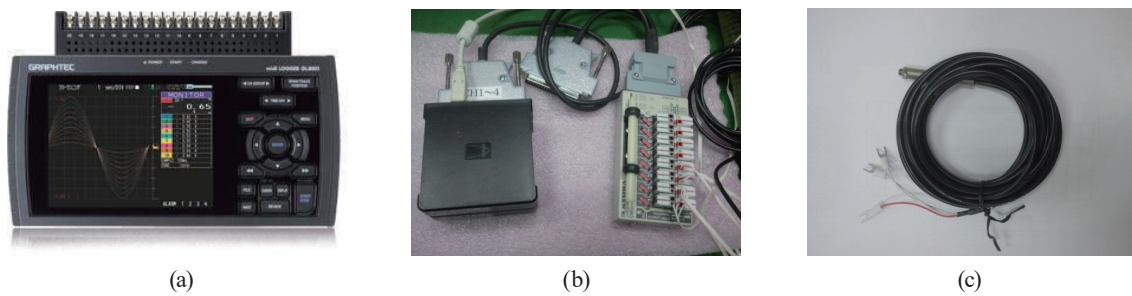


Fig. 2. (Color online) Measurement equipment: (a) signal recorder (GL820), (b) strain module, and (c) PT100.

The MTBF for a series of systems is

$$MTBF_s = \frac{1}{\sum_{i=1}^n \lambda_i} = \frac{1}{\frac{1}{MTBF_1} + \frac{1}{MTBF_2} + \dots + \frac{1}{MTBF_n}}. \quad (3)$$

From the structural deformation of the single-axis feed platform and the heat-induced thermal expansion of the material, we can obtain the deformation simultaneously affected by the stress and temperature using the principle of superposition. Therefore, when the single-axis feed platform is subjected to stress and temperature effects at the same time, the strain in the  $x$  direction can be obtained from this principle as

$$\varepsilon_{xx} = \frac{\sigma_{xx} - \nu(\sigma_{yy} + \sigma_{zz})}{E} + \alpha \cdot T, \quad (4)$$

where  $E$  is Young's modulus (the coefficient of elasticity),  $\nu$  is Poisson's ratio, and  $\sigma$  is the stress. In addition, when the stress and temperature effects occur simultaneously, the unidirectional strain can be obtained from the same principle.

The heat dissipation ability of the cooling oil from the single-axis feed platform is calculated as

$$\dot{Q} = \dot{m}C_p(T_o - T_i), \quad (5)$$

where  $\dot{Q}$  is the cooling capacity,  $\dot{m}$  is the cooling oil flow rate,  $C_p$  is the specific heat of the cooling oil,  $T_o$  is the temperature of the cooling oil outlet of the plate heat exchanger, and  $T_i$  is the temperature of the cooling oil temperature inlet of the plate heat exchanger.

### 2.3 Research method

The reliability of electronic equipment is improving rapidly, but the concept of reliability for machine tools has not been popularized. Reliability engineering is difficult to implement since

mechanical equipment is a highly integrated electromechanical system. Reliability work begins with the functional specification and evaluation of the cooling system. In this study, the cooling system was used to develop appropriate reliability analysis processes and reliability application technologies. Figure 3 is a flowchart used for estimating the reliability of a cooling system in this study. The MTBF can be calculated using the reliability estimation process. The system's reliability is improved by following reliability design rules.

### 3. Results and Discussion

The cooling system is optimized to prevent unpredictable thermal deformation during the operation of a single-axis feed system. The oil circulating in the cooling system removes the heat generated in a machine tool, thus reducing the thermal deformation of the structure. Reliability engineering is very important for ensuring the stability of machine tools, but it is not easy to implement. Therefore, reliability work starts with considering the cooling system to establish a process suitable for reliability analysis.

#### 3.1 Reliability of cooling system

In this study, we aimed to improve the reliability of a machine tool cooling system and stabilize the structure temperature. To this end, we first created a function block diagram of the cooling system for reliability (Fig. 4). Then, we calculated the reliability from the important parts of the cooling system to obtain the final MTBF.

The oil was cooled to the required temperature by a frequency conversion cooling system. The cooling oil was supplied to the cooling channel of the single-axis machine and the flow was controlled using a solenoid valve to stabilize the temperature of the structure. The set oil temperature, pipeline flow, and structure temperature of the cooling system were monitored to maintain the required conditions.

The cooling system is divided into two units: the cooling unit and the flow adjustment unit. The cooling unit is a standard item, with the model and specifications selected on the basis of the required cooling capacity. The accuracy of temperature control in the cooling system can reach  $\pm 0.1$  °C. The flow adjustment unit uses a flow proportional valve to adjust the flow range to 0.3–10 L/min. All parts and components are arranged in series. Figure 5 shows the reliability block diagram of the system.

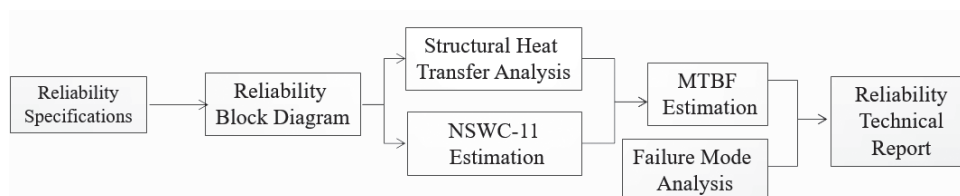


Fig. 3. Reliability method.



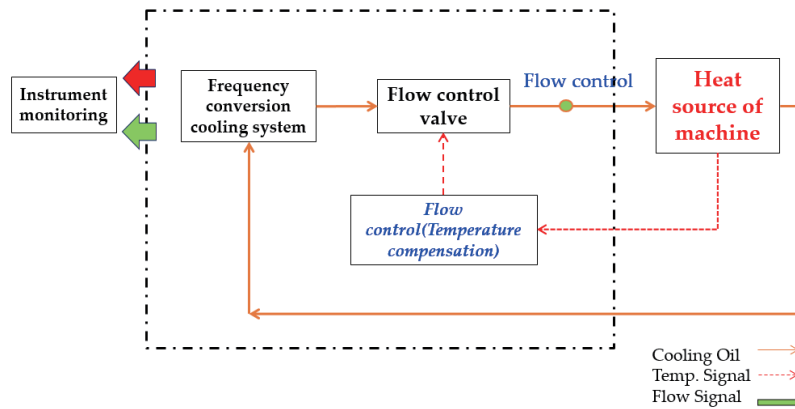


Fig. 4. (Color online) Function block diagram of the cooling system.

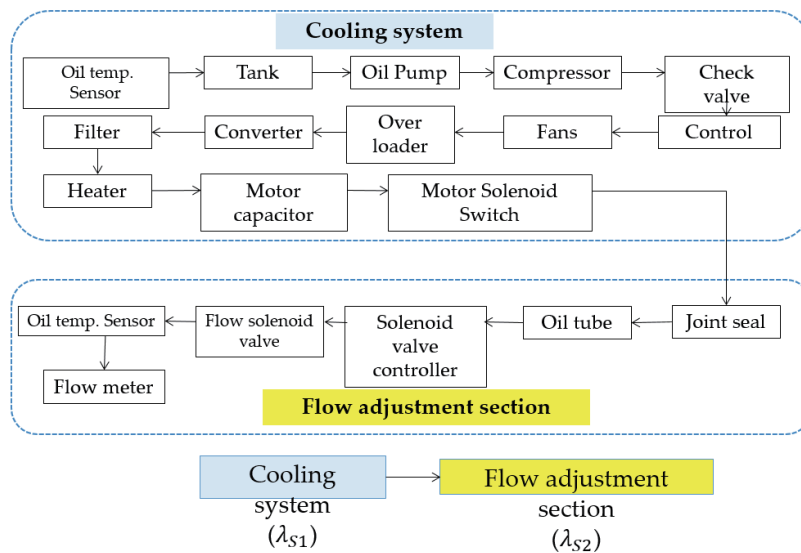


Fig. 5. (Color online) Reliability block diagram of cooling system.

Most parts of the cooling system are purchased products. The manufacturer provides the reliability value and related data about conditions of use, so each product must be used within the limits of its conditions of use. The US Navy reliability specification NSWC-11<sup>(20)</sup>, hydraulic reliability and fault diagnosis, and ALD MTBF calculation software are used as tools to estimate the failure rate of each item. Table 1 shows the product lifetime data of the important outsourced parts. The calculated failure rate of the cooling system is more reliable than the product lifetime data.

In the failure rate calculation, we use the static seal, proportional valve, and filter as examples. The calculation process for each part is presented below.

Table 1  
(Color online) Lifetimes of cooling system parts.

Item	Life	Specification	Used Conditions
Conversion Cooling System	5 years (by supplier)	<ul style="list-style-type: none"> <li>Capacity: 6000 kcal/hour</li> <li>Max flow: 30 L/min</li> <li>Refrigerant: R410a</li> <li>Oil temp: ≤50 °C</li> <li>oil viscosity: 2-300 CST</li> <li>Use hydraulic oil, do not use others</li> <li>Ambient temperature: 10-50 °C</li> </ul>	<ol style="list-style-type: none"> <li>Oil temp: ≤40 °C</li> <li>Ambient temperature: 15-30 °C</li> <li>Keep the oil level of the tank above 80%</li> <li>Clean the filter regularly (6 months)</li> <li>ISO VG22 viscosity 22.8 CST@40 °C ; 4.4 CST@100 °C</li> </ol>
Flow meter	5 years (by supplier)	<ul style="list-style-type: none"> <li>Accuracy: 0.1 L/min</li> <li>Measurement range: 0-50 L/min</li> <li>Anti-magnetic field interference: 1500 Gaussian</li> <li>Ambient temperature: 10-55 °C</li> <li>Environment humidity: 25-85 RH</li> </ul>	<ol style="list-style-type: none"> <li>Flow rate range: 0-3L/min</li> <li>Ambient Temp.: 15-30 °C</li> <li>Environment Humidity: 60RH</li> </ol>
Solenoid valve controller	5 years (by supplier)	<ul style="list-style-type: none"> <li>Ambient temperature: 0-70 °C</li> <li>Voltage: 24 V(21-28 V)</li> <li>Voltage range: 0-10 V</li> <li>Position controlled(PID)</li> <li>Fast power-on and power-off operation</li> <li>Adjustable parameter: Zero point, gain, acceleration gain, deceleration gain</li> </ul>	<ol style="list-style-type: none"> <li>Ambient Temp.: 15-30 °C</li> <li>Flow rate range: 0.3-10L/min</li> <li>Feedback temperature signal controls the position of electromagnetic proportional valve</li> </ol>

Term	Parts	Initial Failure rate(λ) (time/hours)	Final Failure rate(λ) (time/hours)	Verification methods				Data Source
				Simulation	Estimation	Test	Reference data	
1	Tank	1.5x10 <sup>-6</sup>	1.5x10 <sup>-6</sup>				○	Hydraulic reliability and fault diagnosis
2	Filter	1.5x10 <sup>-6</sup>	8.04x10 <sup>-7</sup>				○	NSWC-11
3	Overload device	7.2x10 <sup>-6</sup>	7.2x10 <sup>-6</sup>				○	ALD MTBF Calculator
4	Check valve	5x10 <sup>-6</sup>	5x10 <sup>-6</sup>				○	Hydraulic reliability and fault diagnosis
7	Joint seal	1.87x10 <sup>-6</sup>	0.34x10 <sup>-6</sup>				○	NSWC-11
8	Compressor motor	12.87x10 <sup>-6</sup>	3.27x10 <sup>-6</sup>				○	NSWC-11
9	Fan motor	6.88x10 <sup>-6</sup>	1.42x10 <sup>-6</sup>				○	Hydraulic reliability and fault diagnosis
10	Inverter	20.54x10 <sup>-6</sup>	17.03x10 <sup>-6</sup>				○	ALD MTBF Calculator
11	Tubing	4.42x10 <sup>-6</sup>	4.42x10 <sup>-6</sup>				○	Fundamentals of Hydraulic Reliability Engineering
12	Heater	1.54x10 <sup>-6</sup>	0.7x10 <sup>-6</sup>				○	NSWC-11
13	Oil temp. sensor	0.24x10 <sup>-6</sup>	0.01x10 <sup>-6</sup>				○	ALD MTBF Calculator
14	Controller	18.03x10 <sup>-6</sup>	1.15x10 <sup>-6</sup>				○	Supplier
15	Capacitor	0.7x10 <sup>-6</sup>	0.7x10 <sup>-6</sup>				○	ALD MTBF Calculator
16	Electromagnetic valve	4.62x10 <sup>-6</sup>	0.82x10 <sup>-6</sup>				○	NSWC-11
17	Pump	11.23x10 <sup>-6</sup>	0.12x10 <sup>-6</sup>				○	NSWC-11
18	Filter	0.2x10 <sup>-6</sup>	0.2x10 <sup>-6</sup>				○	ALD MTBF Calculator
19	Solenoid switch	4.36x10 <sup>-6</sup>	4.36x10 <sup>-6</sup>				○	ALD MTBF Calculator

### 3.1.1 Reliability of static seal (see NSWC-11 failure rate model)

The failure rate model of the static seal requires correction coefficients. The failure rate model can be expressed as

$$\lambda_{SE} = \lambda_{SE,B} \cdot C_P \cdot C_{DL} \cdot C_H \cdot C_F \cdot C_v \cdot C_T \cdot C_N, \tag{6}$$

where

- Basic failure rate  $\lambda_{SE,B} = 2.4 \times 10^{-6}$ ,
- Fluid pressure correction coefficient  $C_P: 0.25 (P_s = 72.5 \leq 1500 \text{ lbs/in}^2)$ ,
- Seal size and form correction coefficient  $C_{DL} = 1.1D_{SL} + 0.32 = 19.57$ ,
- Contact stress correction coefficient  $C_H = \left( \frac{M/C}{0.55} \right)^{4.3} = 14.84$ ,
- Contact surface smoothness correction coefficient  $C_F = 0.25$  for  $f \leq 15 \mu\text{in}$ ,
- Fluid viscosity correction coefficient  $C_v = \nu_0/\nu = 0.15$ ,
- Operating temperature correction coefficient  $C_T = 0.21$  for  $(T_R - T_O) > 40 \text{ }^\circ\text{F}$ ,
- Contaminant correction coefficient  $C_N = (C_0/C_{10})^3 = 1.365$  and,
- Failure rate of static seal  $\lambda_{SE} = 0.345 \times 10^{-6}$  (time/h).

### 3.1.2 Reliability of proportional valve (refer to NSWC-11 failure rate model)

The failure rate model of the proportional valve also requires correction coefficients. The failure rate model can be expressed as

$$\lambda_{SO} = \lambda_{SO,B} \cdot C_T \cdot C_K \cdot C_S, \tag{7}$$



where

Basic failure rate	$\lambda_{SO,B} = 2.77 \times 10^{-6}$ ,
Temperature correction coefficient	$C_T = (1/1.5)^3 = (1/1.5^{0.5})^3 = 0.54$ ,
Application mode correction coefficient (database)	$C_K = 1.1$ ,
Usage frequency correction coefficient (number of operations/h) (database)	$C_S = 0.5$ , and
Failure rate of proportional valve	$\lambda_{SO} = 0.82 \times 10^{-7}$ (time/h).

### 3.1.3 Reliability of filter (refer to NSWC-11 failure rate model)

The failure rate model of the filter also requires correction coefficients and can be expressed as

$$\lambda_F = \lambda_{FB} \cdot C_{DP} \cdot C_V \cdot C_{CS} \cdot C_{CF}, \quad (8)$$

where

Basic failure rate	$\lambda_{SE,B} = 2.53 \times 10^{-6}$ ,
Pressure correction coefficient	$C_{DP} = 1.25 * (P_O/P_R)^x$ ,
Vibration amplification coefficient (database)	$C_V = 1$ ,
Cold start correction coefficient	$C_{CS} = (v_{cold}/v_{op})^x = (103/96)^{0.2} = 1.01$ ,
Circulation flow correction coefficient	$C_{CF} = 0.15$ (coarse filter), and
Failure rate of the filter	$\lambda_F = 8.04 \times 10^{-7}$ (time/h).

## 3.2 Prediction of reliability

The MTBF of the cooling system can be preliminarily calculated through the reliability estimation process in Fig. 6, and the cooling system reliability is improved to the target value by applying the reliability design rules. The failure rates of all parts and components and the lifetime data provided by the manufacturer are integrated and substituted in the reliability model of the series system expressed as Eq. (3) to obtain the MTBF of the entire cooling system. The calculation results are as follows:

Cooling system	$\lambda_{s1} = 0.000026$ (time/h), MTBF = $1/\lambda_{s1} = 15151$ h,
Flow adjustment device	$\lambda_{s2} = 0.0000174$ (time/h), MTBF = $1/\lambda_{s2} = 57471$ h,
Single-axis cooling system	$\lambda_s = \lambda_{s1} + \lambda_{s2} = 0.000026 + 0.0000174 = 0.0000434$ , and MTBF = $1/\lambda_s = 23041$ .

The MTBF of the cooling system was improved from 3787 to 23,041 h by reliability engineering methods.

## 3.3 Simulation and experiment of cooling system

We used the orthogonal array of the Taguchi method to perform the finite element analysis of the preliminary design of the single-axis feed platform and to analyze the parameter planning.

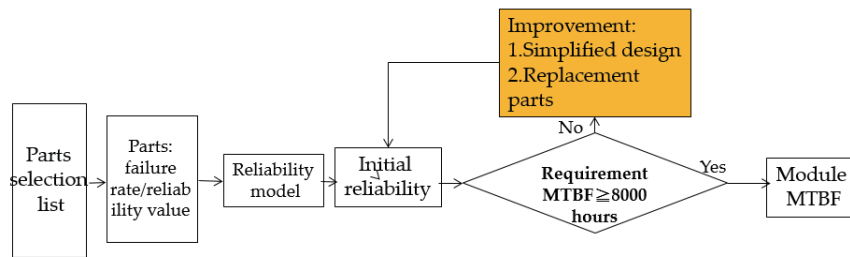


Fig. 6. (Color online) Reliability estimation process.

The orthogonal array is improved from that of the full factorial experimental method, which is very inefficient and has an excessive experimental cost. The Taguchi orthogonal array is an important tool for reducing the experimental cost while maintaining accuracy. Before using the Taguchi method to simulate the cooling flow channel conditions, we found several control factors that considerably affect the cooling efficiency. Tables 2 and 3 show a screening table of the factors expected to affect the structure temperature and the  $L_{16}(4^5)$  orthogonal array, respectively. The possible factors affecting the cooling efficiency must be screened using a simple method based on cost considerations to determine the important factors, because incorrectly selected or repeated factors would reduce the effectiveness of the experiment.

The Taguchi method is used to plan the parameters for the verification of vehicle design. Finite element analysis software is used for cooling channel analysis. The design parameters of the important factors that affect the structure temperature are found through the experimentally designed orthogonal array and variation analysis. Figure 7 is the simulation analysis diagram in the study. The mesh method is automatically generated by software and the orthogonality of mesh quality is  $>0.1$  or above. The red part is the setting of the cooling channel. The diameter of the circular cooling channel is 25.4 mm and the square cooling channel is 200 mm\*50 mm. In the heat exchange mode, cooling oil is used to take away the heat energy generated during the operation of the single-axis feed platform.

In this study, the signal-to-noise ( $S/N$ ) ratio is used as a quality indicator. The expected variation of the structure temperature is  $23 \pm 0.5$  °C. The required quality characteristic is that a smaller accuracy error is better. The statistical smaller-the-better formula is used to calculate the  $S/N$  ratio. The response values of the  $S/N$  ratio and quality characteristic factors at various levels in Table 3 are observed to determine the optimal cooling parameters. The variation of each factor between different levels is observed, then the variations of the parameters are subtracted to observe the sensitivity of each factor. When its sensitivity is high, a factor is considered important, and when its sensitivity is not obvious, a factor is considered unimportant. Finally, a set of optimal cooling parameters is obtained, as shown in Table 4.

Multivariate regression analysis is used to statistically analyze the sampling temperature and thermal deformation to establish a mathematical relationship between the temperature increase and the thermal error at a specific point. The sampling temperature point and thermal deformation must have a significant correlation for the data to be processed. The position set for

Table 2  
Screening table of factors affecting structure temperature.

Body isotherm factor screening table				
	Major effect	Easy to operate and control	Cost-effective and economical	Easy to predict
a. Oil heat transfer coefficient	v	v	v	v
b. Ambient temperature	v			v
c. Ambient humidity	v			v
d. Cooling channel diameter	v	v	v	v
e. Cooling flow	v	v	v	v
f. Cooling temperature	v	v	v	v
g. Structural material composition			v	v
h. Oil fluidity	v	v	v	v
i. Feeding velocity	v	v		v
j. Feed stroke	v	v		

Table 3  
Orthogonal array.

Factor	Level				Unit
A. Flow rate	1.5	2	2.5	3	L/min
B. Temperature	19	20	21	22	°C
C. Tube dimension	14	16	18	20	mm
D. Coolant heat transfer coefficient	60	122	198	250	W/m <sup>2</sup> ·m
E. Coolant fluidity	2.1	4.8	9.9	15	Pa·S

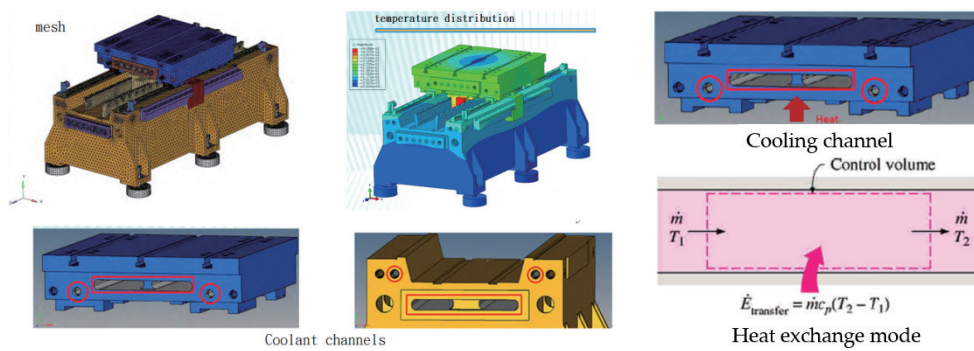


Fig. 7. (Color online) Simulation analysis.

Table 4  
Optimal cooling parameters.

A. Flow	B. Temperature	C. Tube diameter	D. Oil heat transfer coefficient	E. Oil fluidity
A2	B2	C4	D1	E2
2 (L/min)	20 (°C)	20 (mm)	60 (W/m <sup>2</sup> ·K)	4.8 (Pa·S)

the temperature point will directly affect the accuracy of the regression equation. Figure 8(a) shows the result of our preliminary experiment, where the temperature change is  $\pm 0.943$  °C. Figure 8(b) shows the result obtained after multivariate regression analysis is used in the experiment. The temperature variation of the structure is reduced to less than  $\pm 0.517$  °C.

The set of cooling parameters obtained using the Taguchi method (Table 3) is reintroduced into the verification platform to conduct the cooling experiment. The structural thermal equilibrium temperature variation of multivariate regression analysis decreases from  $\pm 0.517$  to  $\pm 0.465$  °C, a reduction of 10.1%, as shown in Fig. 9.

The experiment revealed the optimal cooling conditions shown in Table 4. The five control factors are a flow rate of 2 L/min, a cooling temperature of 20 °C, a cooling channel diameter of 20 mm, an oil heat transfer coefficient of 60 w/m<sup>2</sup>.K, and an oil fluidity of 4.8 Pa·S. However, to

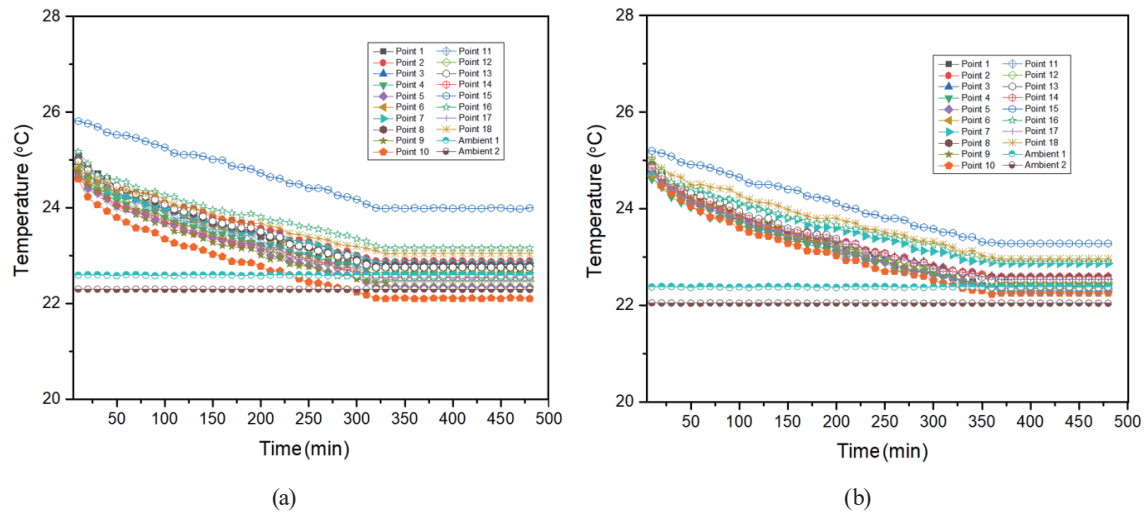


Fig. 8. (Color online) Results of cooling experiment: (a) preliminary results and (b) results of multivariate regression analysis.

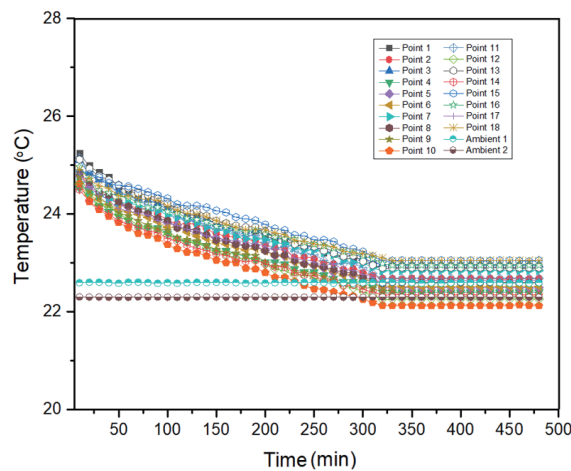


Fig. 9. (Color online) Structural temperature of cooling obtained with the Taguchi method.

obtain cooling conditions better than those in Table 4, the tolerance design is used in the cooling experiment again. An increase in cost usually accompanies tolerance design. However, in the experiment in this study, we only made slight adjustments to the upper and lower limits of the variations of the flow, temperature, and tube diameter among the cooling parameters (as shown in Table 4). We selected a suitable orthogonal array to perform another experiment using the Taguchi method, then selected the levels with the best values of the control factors within each variation range. The optimized process was matched to the factor level table after this experiment to obtain the optimal operating parameters.

The  $L_9(4^3)$  orthogonal array was used in the experiment on tolerance design. Each experiment was performed twice, and the average value, standard deviation, and  $S/N$  ratio (smaller-the-better characteristic) were obtained. After normalizing the data, a confirmation table for the optimal cooling parameters after the tolerance setting was obtained. Finally, the  $S/N$  ratios corresponding to each factor at three levels were averaged, as shown in Table 5. Finally, the optimal cooling parameters after the tolerance design were obtained, factor A at L2, factor B at L3, and factor C at L3, as shown in Table 6.

Table 5  
Control factor levels for tolerance design.

	L1	L2	L3	Unit
A. Flow	1.75	2	2.25	L/min
B. Temperature	19.5	20	20.5	°C
C. Tube diameter	19	20	21	mm

Table 6  
Optimal cooling parameters after tolerance design.

A. Flow	B. Temperature	C. Tube diameter	D. Oil heat transfer coefficient	E. Oil fluidity
L2	L3	L3	D1	E2
2 (L/min)	20.5 (°C)	21 (mm)	60 (W/m <sup>2</sup> ·K)	4.8 (Pa·S)

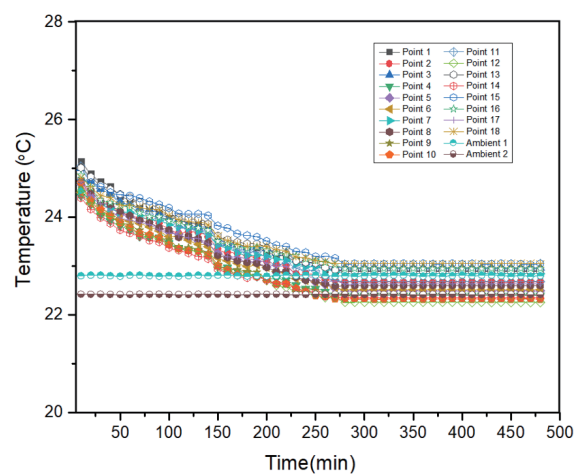


Fig. 10. (Color online) Experimental results of optimized cooling parameters.

The final experiment verified the optimal cooling parameters, and the entire original process was compared with the optimal process to minimize the variation of the structure temperature. The experimental results with the optimized cooling parameters are shown in Fig. 10. The temperature change in the structural thermal balance is reduced from  $\pm 0.465$  to  $\pm 0.367$  °C, a decrease of 21.1%.

#### 4. Conclusions

We used the reliability engineering technique to develop a cooling control system, simplify the design method, and improve the cooling system. The MTBF of the cooling system was increased from 3,787 h to more than 23,041 h. When the Taguchi method was used in the design of experiments on structural cooling, the number of experiments and their cost were reduced, thus simplifying the data analysis. Additionally, the technical research indicators, such as cooling temperature control, machining accuracy, and thermal suppression method, can be improved using the tolerance design method. Finally, the main conclusions are as follows:

1. In the technology development process, reliability engineering is applied to enhance the MTBF of a cooling system to maintain the structure temperature.
2. Using the Taguchi method with the finite element method and multivariate regression analysis, we found the best cooling channels and conditions, which were verified by experimental data.
3. The temperature variation of the structure was reduced from  $\pm 0.517$  to  $\pm 0.367$  °C, a decrease of 29%.

#### Acknowledgments

The authors gratefully acknowledge the financial support provided to this study by the Ministry of Science and Technology of Taiwan under Grant MOST 110-2222-E-167-001-MY3.

#### References

- 1 J. Bryan: CIRP Ann. **39** (1990) 645. [https://doi.org/10.1016/S0007-8506\(07\)63001-7](https://doi.org/10.1016/S0007-8506(07)63001-7)
- 2 J. Vyroubal: Precis. Eng. **36** (2012) 121. <https://doi.org/10.1016/j.precisioneng.2011.07.013>
- 3 Y. H. Huang, C. W. Huang, Y. D. Chou, C. C. Ho, and M. T. Lee: Smart Sci. **4** (2016) 160. <https://doi.org/10.1080/23080477.2016.1214062>
- 4 T. Liu, W. Gao, Y. Tian, H. Zhang, W. Chang, K. Mao, and D. Zhang: Appl. Therm. Eng. **76** (2015) 54. <https://doi.org/10.1016/j.applthermaleng.2014.10.088>
- 5 T. T. Ngo, C. C. Wang, Y. T. Chen, and V. T. Than: Therm. Sci. Eng. Prog. **25** (2021) 100958. <https://doi.org/10.1016/j.tsep.2021.100958>
- 6 K. Y. Li, W. J. Luo, X. H. Hong, S. J. Wei, and P. H. Tsai: IEEE Access **8** (2020) 28988. <https://doi.org/10.1109/ACCESS.2020.2972580>
- 7 Y. Tang, X. Jing, W. Li, Y. He, and J. Yao: Appl. Therm. Eng. **198** (2021) 117478. <https://doi.org/10.1016/j.applthermaleng.2021.117478>
- 8 C. Xia, J. Fu, J. Lai, X. Yao, and Z. Chen: Appl. Therm. Eng. **90** (2015) 1032. <https://doi.org/10.1016/j.applthermaleng.2015.07.024>
- 9 Y. Dai, J. Wang, Z. Li, G. Wang, X. Yin, X. Yu, and Y. Sun: Case Studies in Thermal Engineering **26** (2021) 101056. <https://doi.org/10.1016/j.csite.2021.101056>
- 10 A. Z. Keller, A. R. R. Kamath, and U. D. Parera: Reliab. Eng. **3** (1982) 449. [https://doi.org/10.1016/0143-8174\(82\)90036-1](https://doi.org/10.1016/0143-8174(82)90036-1)



- 11 Y. Ran, W. Zhang, Z. Mu, and G. Zhang: Reliab. Maint. (2019). <https://doi.org/10.5772/intechopen.85163>
- 12 Z. Wang, Y. Ran, H. Yu, S. Zhang, and G. Zhang: Int. J. Adv. Manuf. Technol. **107** (2020) 2767. <https://doi.org/10.1007/s00170-020-05168-2>
- 13 H. Li, Z. M. Deng, N. A. Golilarz, and C. G. Soares: Reliab. Eng. Syst. Saf. **215** (2021) 107846. <https://doi.org/10.1016/j.res.2021.107846>
- 14 Z. Zhang, L. Cai, Q. Cheng, Z. Liu, and P. Gu: J. Int. Manuf. **30** (2019) 495. <https://doi.org/10.1007/s10845-016-1260-8>
- 15 O. Anikeeva, A. Ivakhnenko, and A. Zhirkov: Procedia Eng. **150** (2016) 712. <https://doi.org/10.1016/j.proeng.2016.07.092>
- 16 Q. Cheng, Z. Zhang, G. Zhang, P. Gu, and L. Cai: J. Mech. Eng. Sci. **229** (2014). <https://doi.org/10.1177/0954406214542491>
- 17 Z. Zhang, Y. Yang, G. Li, C. Yue, Y. Hu, and Y. Li: Int. J. Adv. Manuf. **124** (2023) 4057. <https://doi.org/10.1007/s00170-022-08832-x>
- 18 J. Guo, D. Wang, W. Chen, and R. Fan: IEEE/ASME Trans. Mechatron. **23** (2018) 1930. <https://doi.org/10.1109/TMECH.2018.2841883>
- 19 Y. Liu, H. Peng, and Y. Yang: Appl. Sci. **9** (2019). <https://doi.org/10.3390/app9010014>
- 20 Handbook of Reliability Prediction Procedures for Mechanical Equipment NSWC 11, ISBN 978-82-14-04830-8, Naval Surface Warfare Center.

## About the Authors



**Kun-Ying Li** was born in Chiayi, Taiwan in 1979. He received his B.S. degree from the Department of Bio Mechatronics Engineering, National Chung Hsing University and his M.S. degree from the Department of Mechanical Engineering, National Chung Cheng University, Taiwan, in 2007. From 2007 to 2020, he was an engineer with the Intelligent Machinery Technology Center, Industrial Technology Research Institute. He received his Ph.D. degree from National Chin-Yi University of Technology, Taiwan, in 2020. He has been an assistant professor of the Intelligent Automation Engineering Department, National Chin-Yi University of Technology, Taiwan, since 2020. His research interests include thermal errors of machine tools, design for precision machinery, and reliability engineering applications. He holds 15 patents in machine tools. ([likunying@ncut.edu.tw](mailto:likunying@ncut.edu.tw))



**Chun-Hao Chen** was born in Changhua, Taiwan, in 1979. He obtained a master's degree from the Department of Mechatronic Engineering, National Taiwan Normal University, Taiwan, in 2006. He is currently studying under a doctoral program at National Chin-Yi University of Technology. His research interests are in digital signal processing, industrial robot applications, and machine tool design technology. ([jjcalchen@expetech.com.tw](mailto:jjcalchen@expetech.com.tw))